Biochemical and Biophysical Research Communications 606 (2022) 61–67

Contents lists available at ScienceDirect

Biochemical and Biophysical Research Communications

journal homepage: www.elsevier.com/locate/ybbrc

# Pro-inflammatory polarization of macrophages is associated with reduced endoplasmic reticulum-mitochondria interaction

Leandro Henrique de Paula Assis [a], Gabriel de Gabriel Dorighello [a, b], Helena Coutinho Franco de Oliveira [a, *]

[a] Department of Structural and Functional Biology, Institute of Biology, State University of Campinas, SP, 13083-872, Brazil
[b] Department of Pathology, Faculty of Medical Sciences, State University of Campinas, Campinas, SP, 13083-872, Brazil

ARTICLE INFO

*Article history:*
Received 8 March 2022
Accepted 16 March 2022
Available online 17 March 2022

*Keywords:*
Macrophage
Endoplasmic reticulum-mitochondria interaction
Mitochondrial respiration
Oxidants production

ABSTRACT

Macrophages play a role in host defense, tissue remodeling and inflammation. Different inflammatory stimuli drive macrophage phenotypes and responses. In this study we investigated the relationship between macrophages immune phenotype and mitochondrial bioenergetics, cell redox state and endoplasmic reticulum (ER)-mitochondria interaction. Bacterial lipopolysaccharide (LPS) and interferon-γ (IFNγ) pro-inflammatory stimuli decreased oxidative metabolism (basal, phosphorylating and maximal conditions) and increased baseline glycolysis (117%) and glycolytic capacity (43%) in THP-1 macrophages. In contrast, interleukin-4 (IL4) and interleukin-13 (IL13) anti-inflammatory stimuli increased the oxygen consumption rates in baseline conditions (21%) and associated with ATP production (19%). LPS + IFNγ stimuli reduced superoxide anion levels by accelerating its conversion into hydrogen peroxide ($H_2O_2$) while IL4+IL13 decreased $H_2O_2$ release rates. The source of these oxidants was extra-mitochondrial and associated with increased NOX2 and SOD1 gene expression. LPS + IFNγ stimuli decreased ER-mitochondria contact sites as measured by IP3R1-VDAC1 interaction (34%) and markedly upregulated genes involved in mitochondrial fusion (9–10 fold, MFN1 and 2) and fission (~7 fold, DRP1 and FIS1). Conversely, IL4+IL13 stimuli did not altered ER-mitochondria interactions nor MFN1 and 2 expression. Together, these results unveil ER-mitochondria interaction pattern as a novel feature of macrophage immunological, metabolic and redox profiles.



## 1. Introduction

Macrophages are key cells involved in acute and chronic inflammation. They may develop a wide range of phenotypes depending on the microenvironment and specific stimuli. These cells contribute to repair, resolve or perpetuate an inflammatory condition. Besides, macrophage responses go beyond immunity and affects both metabolic and cardiovascular diseases.

IFNγ, TNFα and toll-like receptor (TLR) ligands - such as lipopolysaccharide (LPS) from gram-negative bacteria - polarize macrophages towards the M1 state. This pro-inflammatory phenotype is related with bactericidal and phagocytic functions. M1 macrophages use glycolysis as the main source of ATP and secrete high levels of pro-inflammatory cytokines, such as IL6, IL12 and TNFα. In contrast, IL4 and IL13 stimuli drive macrophage polarization towards the M2 state, which present wound healing and tissue repair functions. M2 macrophages use oxidative phosphorylation to sustain energy cellular demands and produce high levels of anti-inflammatory cytokines, including IL10 and TGFβ [1]. Although M1 and M2 phenotypes only exist in controlled in vitro experiments, they are useful tools to study macrophage properties in distinct physiological conditions. Other macrophage phenotypes include the M4, Mox, Mhem and M(Hb) states [2].

The interaction between ER and mitochondria plays a role in inflammatory diseases [3]. Recent reports show rheumatoid arthritis, coronary artery disease [4] and hypercholesterolemia [5] change ER-mitochondria interaction pattern in macrophages, which affect overall cell signaling and cellular functions. Based on that, we hypothesized changes in the ER-mitochondria interaction might participate in the macrophage immunometabolic pattern

* Corresponding author.Department of Structural and Functional Biology, Institute of Biology, State University of Campinas, R. Monteiro Lobato, 255, Campinas, 13083-862, SP, Brazil.
*E-mail addresses:* lhpassis@unicamp.br (L.H.P. Assis), ggtdorig@unicamp.br (G.G. Dorighello), ho98@unicamp.br (H.C.F. Oliveira).

https://doi.org/10.1016/j.bbrc.2022.03.086
0006-291X/

switch. Thus, we investigated the potential relationship between macrophages immune phenotype (naïve M0 and M1 or M2 polarized macrophages) and mitochondrial bioenergetics and dynamics, cell redox state and ER-mitochondria interaction.

## 2. Material and methods

### 2.1. Cell culture

THP-1 monocytes (ATCC, TIB-202, Manassas, VA) were kept in RPMI-1640 medium (Vitrocell, Campinas, BR) containing 10 mM HEPES pH 7.4, 1 mM sodium pyruvate, 25 mM glucose and 10% (v/v) fetal bovine serum (Vitrocell) at 37 °C and 5% (v/v) $CO_2$. Monocytes were differentiated into naïve macrophages (M0) using 150 ηM phorbol 12-myristate 13-acetate (PMA, Sigma-Aldrich, St. Louis, MO) for 24 h. Next, macrophages rested in a complete fresh medium for additional 24 h. To polarize in the M1 state, macrophages were incubated with 20 ηg/ml interferon-γ (IFNγ, Abcam, Cambridge, UK) and 1 ηg/ml lipopolysaccharide (LPS) from *Escherichia coli* O111:B4 (Sigma-Aldrich). To polarized in the M2 state, macrophages were incubated with 20 ηg/ml interleukin-4 (IL4, Sigma-Aldrich) and 20 ηg/ml interleukin-13 (IL13, Sigma-Aldrich) [6]. Polarization followed for 24 or 48 h.

### 2.2. Gene expression

THP-1 cells were seeded at 150,000 cells/well in a 24-well plate (Nest Biotechnology, Wuxi, CN), differentiated and polarized as described above. Total RNA was extracted using TRIzol reagent (ThermoFisher Scientific, Waltham, MA) and quantified in NanoDrop spectrophotometer (ThermoFisher Scientific). Two micrograms of total RNA were reverse transcribed using High-Capacity cDNA Reverse Transcription Kit (Applied Biosystem, Foster City, CA). Amplification step was carried out using Fast SYBR Green Master Mix (ThermoFisher Scientific), 50 ηg cDNA and 300 ηM of each forward and reverse oligonucleotide (Table S1**).** RT- PCR assays were conducted in the 7500 Real-Time PCR System (Applied Biosystems). Results were normalized based on GAPDH gene expression. Relative gene expression was quantified using the $\Delta\Delta C_T$ method [7].

### 2.3. Cytokine secretion

THP-1 cells were seeded at 150,000 cells/well in a 24-well plate (Nest Biotechnology), differentiated and polarized as described above. Cytokine secretion was determined in the culture medium using Human Interleukin-10 Quantikine HS ELISA kit (R&D Systems) and Human IL-1β/IL-1F2 Quantikine HS ELISA kit (R&D Systems, Minneapolis, MN), according to the manufacturer instructions.

### 2.4. Mitochondrial respiration and glycolysis

THP-1 cells were seeded at 250,000 cells/well in a 24-well Seahorse XFe24 cell culture plate (Agilent Technologies, Santa Clara, CA), differentiated and polarized as described above. Macrophages were incubated in a non-buffered RPMI-1640 medium at 37 °C in the absence of phenol red, fetal bovine serum and $CO_2$. Macrophages were analyzed in the Seahorse XFe24 Extracellular Flux Analyzer (Agilent Technologies). The oxygen consumption rates (OCR) associated with different mitochondrial states were assessed using different drugs. This includes 1 μM oligomycin (ATP synthase inhibitor), 1 μM carbonyl cyanide 4-(trifluoromethoxy) phenylhydrazone (FCCP, mitochondrial uncoupler) and a mix of 1 μM antimycin A (complex III inhibitor) plus 1 μM rotenone (complex I inhibitor). Extracellular acidification rates (ECAR) were determined independently of OCR assays, as follows, 11.1 mM glucose was added to the culture medium to stimulate glycolysis and a mix of 1 μM antimycin A plus 1 μM rotenone was used to evaluate the maximal glycolysis activity. OCR and ECAR data were normalized using violet crystal-stained cells.

### 2.5. Superoxide anion production

THP-1 cells were seeded at 75,000 cells/well in a 96-well plate with μClear bottom (Greiner Bio-one, Kremsmünster, AT), differentiated and polarized as described above. Next, the culture medium was replaced and cells were washed with PBS solution (137 mM NaCl, 2.7 mM KCl, 4.3 mM $NaH_2PO_4$, 1.4 mM $KH_2PO_4$ and pH 7.4) at 37 °C. Cells were incubated with 2 μM dihydroethidium (DHE, Thermo Fisher Scientific) or 10 μM mitochondrial superoxide indicator (MitoSOX Red, Thermo Fisher Scientific) diluted in PBS solution at 37 °C, 5% (v/v) $CO_2$ for 10 min. Fluorescence was monitored in a SpectraMax M3 spectrophotometer (Molecular Devices) at 518/605 nm for DHE and 510/580 nm for MitoSOX (excitation/emission wavelength). Results were background-subtracted using non-probed cells.

### 2.6. Hydrogen peroxide production

THP-1 cells were seeded at 250,000 cells/well in a 96-well plate (Greiner Bio-one), differentiated and polarized as described above. Hydrogen peroxide was measured using 25 μM Amplex Red (ThermoFisher Scientific) and 0.2 U/ml Pierce Horseradish Peroxidase (HRP, ThermoFisher Scientific) as previously described [5]. To determine hydrogen peroxide released from non-mitochondrial sources, macrophages were first incubated with 1 μM FCCP [8].

### 2.7. Gene silencing

THP-1 cells were seed at 60,000 cells/well (in a 96-well plate) or 150,000 cell/well (in a 24-well plate) and differentiated as described above. Cells rested for 24 h in complete fresh medium before transfection. M0 macrophages were transfected with 1 ρmol/well (for 96-well plate) or 5 ρmol/well (for 24-well plate) of specific siRNA for VDAC1 (Thermo Fisher Scientific, HSS187665), ITPR1 (Thermo Fisher Scientific, HSS179996) or AllStars Negative Control (Qiagen, 1027281) using Lipofectamine RNAiMAX (Thermo Fisher Scientific). Gene silencing was carried out for 24 h.

### 2.8. Proximity ligation assay (PLA)

THP-1 cells were seeded at 60,000 cells/well in a 96-well plate with a μClear bottom (Greiner Bio-one), differentiated and polarized as described above. Immunocytochemistry and proximity ligation assay (PLA) were performed exactly as previously described [5]. Cells labeled with fluorescent dyes (Cyanine-5 or DAPI) were imaged in the ImageXpress Micro Confocal High Content Imaging System (Molecular Devices), using a CFI Super Plan Fluor ELWD 40X/0.60 (Nikon, 236 MRH08430, Melville, NY) with 0.17 correction collar. Raw images were analyzed in the MetaXpress 6 software using the Transfluor tool (Molecular Devices). Representative images were corrected regarding intensity above background, contrast and brightness using Fiji software [9].

### 2.9. Statistical analyses

Data were expressed as mean ± standard error (SE). Statistical analyses were carried out with Prism 7 (GraphPad, San Diego, CA). Data were compared using a two-tailed unpaired Student t-test

when datasets passed Saphiro-Wilk omnibus normality test (alpha = 0.05). Comparisons among three groups were performed using one-way ANOVA followed by a Bonferroni's post-test. Statistical significance was defined for $p < 0.05$.

## 3. Results

### 3.1. Characterization of M1/M2 macrophage phenotypes

As expected, LPS + IFNγ pro-inflammatory stimuli increased TNFα, IL1β, CXCL10 and CXCL11 gene expression in macrophages 24 h (Fig. 1A) and 48 h (Fig. S1A) after treatment. Because serum may contain oxidized phospholipids, we evaluated the Mox phenotype marker NFE2L2 [10,11]. LPS + IFNγ stimuli upregulated NFE2L2 gene expression 48 h after treatment (Fig. S1A). Following, IL1β secretion increased 62 times 24 h after stimulation and remaining increased after 48 h (Fig. 1B). Regarding the anti-inflammatory IL4+IL13 stimuli, we observed significant increases in IL10, MMR and CCL22 gene expression in macrophages 24 h (Fig. 1C) and 48 h (Fig. S1B) after stimuli, whereas CD163 marker was downregulated 24 h after treatment (Fig. 1C). NFE2L2 gene expression was downregulated 24 and 48 h after stimulation (Fig. 1C, Fig. S1B). Besides, IL10 secretion showed a 2.6-fold increase 48 h after stimulation (Fig. 1D). Therefore, LPS + IFNγ stimuli induce the expression of pro-inflammatory genes and IL1β secretion (M1 phenotype), whereas IL4+IL13 stimuli induce the expression of anti-inflammatory genes and IL10 secretion (M2 phenotype).

### 3.2. Macrophage immunological phenotypes alter their metabolic profile

The three macrophage phenotypes (M0 naïve, M1 pro-inflammatory and M2 anti-inflammatory) were different in terms of oxidative metabolism (Fig. 2A). Mitochondria from M2 macrophages had baseline oxygen consumption rate (OCR) higher than those from M0 (21%) and M1 (69%) (Fig. 2B). OCR linked with ATP synthesis was also higher in M2 than in M0 (19%) and M1 (60%) (Fig. 2C). The maximal stimulated OCR was 68% higher in both M2 and M0 than in M1 (Fig. 2D). Mitochondria from M2 and M0 showed 67% higher spare respiratory capacity than M1 (Fig. 2E). Proton leak was increased in M2 when compared to M0 (28%) and M1 (116%) (Fig. 2F). M0 and M1 states showed 26% higher OCR from non-mitochondria sources than M2 (Fig. 2G). The extracellular acidification rates (ECAR) indicate the glycolytic metabolism (Fig. 2H–K). M1 macrophages showed enhanced baseline glycolytic rate compared with M0 (54%) and M2 (45%) (Fig. 2I). Accordingly, glycolytic capacity was higher in M1 than in M0 (31%) and M2 (28%) (Fig. 2J). Glycolytic reserve was similar among the three phenotypes (Fig. 2K). Together, these results show M2 macrophages use oxidative metabolism as the main energy acquiring process while M1 macrophages are mainly glycolytic.

### 3.3. Pro-inflammatory stimulus induces superoxide anion conversion into hydrogen peroxide

M1 macrophages showed reduced whole-cell superoxide anion levels when compared to M0 (36%) and M2 (46%) (Fig. 3A). Superoxide anion derived from mitochondrial respiration was equivalent among the three phenotypes (Fig. 3B). Total cell (Fig. 3C) and non-mitochondrial (Fig. 3D) hydrogen peroxide release rates were 29% higher in M0 and M1 macrophages than in M2. No significant differences in the hydrogen peroxide released by mitochondria were observed among the three phenotypes (Fig. 3E). Since superoxide anion levels are lower in M1 than M0 and hydrogen peroxide levels are equivalent in M1 and M0, we may conclude that superoxide anion conversion into hydrogen peroxide is stimulated in M1, a hallmark of activated macrophages. Accordingly, cytosolic SOD1 gene expression, but not mitochondrial SOD2, is highly upregulated in M1 macrophages (Fig. 3F).

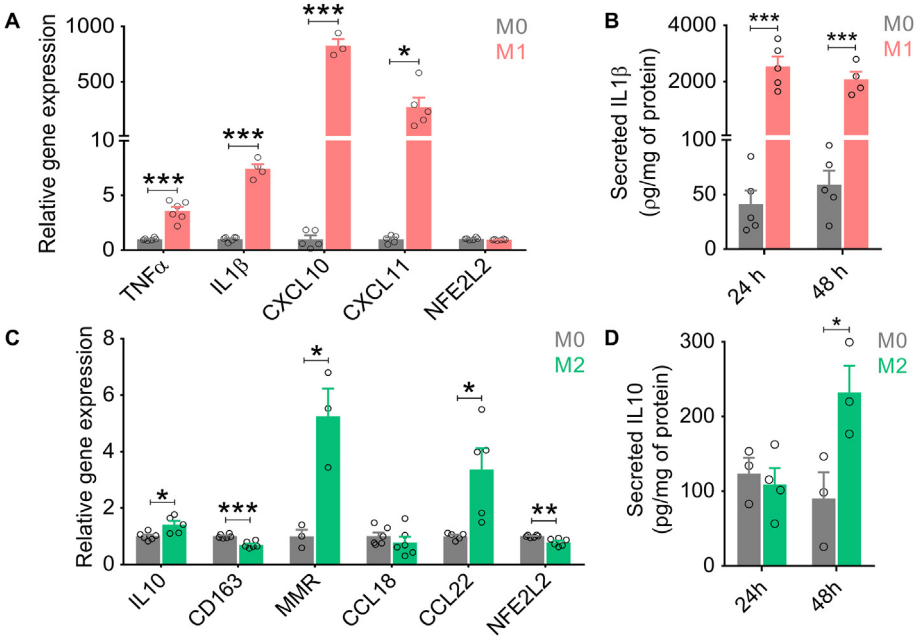


**Fig. 1. LPS + IFNγ stimuli induce M1 macrophage state, whereas IL4+IL13 stimuli induce M2 macrophage state. (A,C)** Relative gene expression of inflammatory markers in naïve (M0) and M1/M2 polarized macrophages 24 h after stimulation. Three to six independent cell batches analyzed in duplicates. **(B,D)** Cytokine secretion 24 and 48 h after stimulation. Three to five independent cell batches analyzed in triplicates. Data are expressed as mean ± SE. Statistical analyses were performed using a two-tailed unpaired Student t-test. *, **, *** with $p < 0.05$, 0.01 and 0.001, respectively.

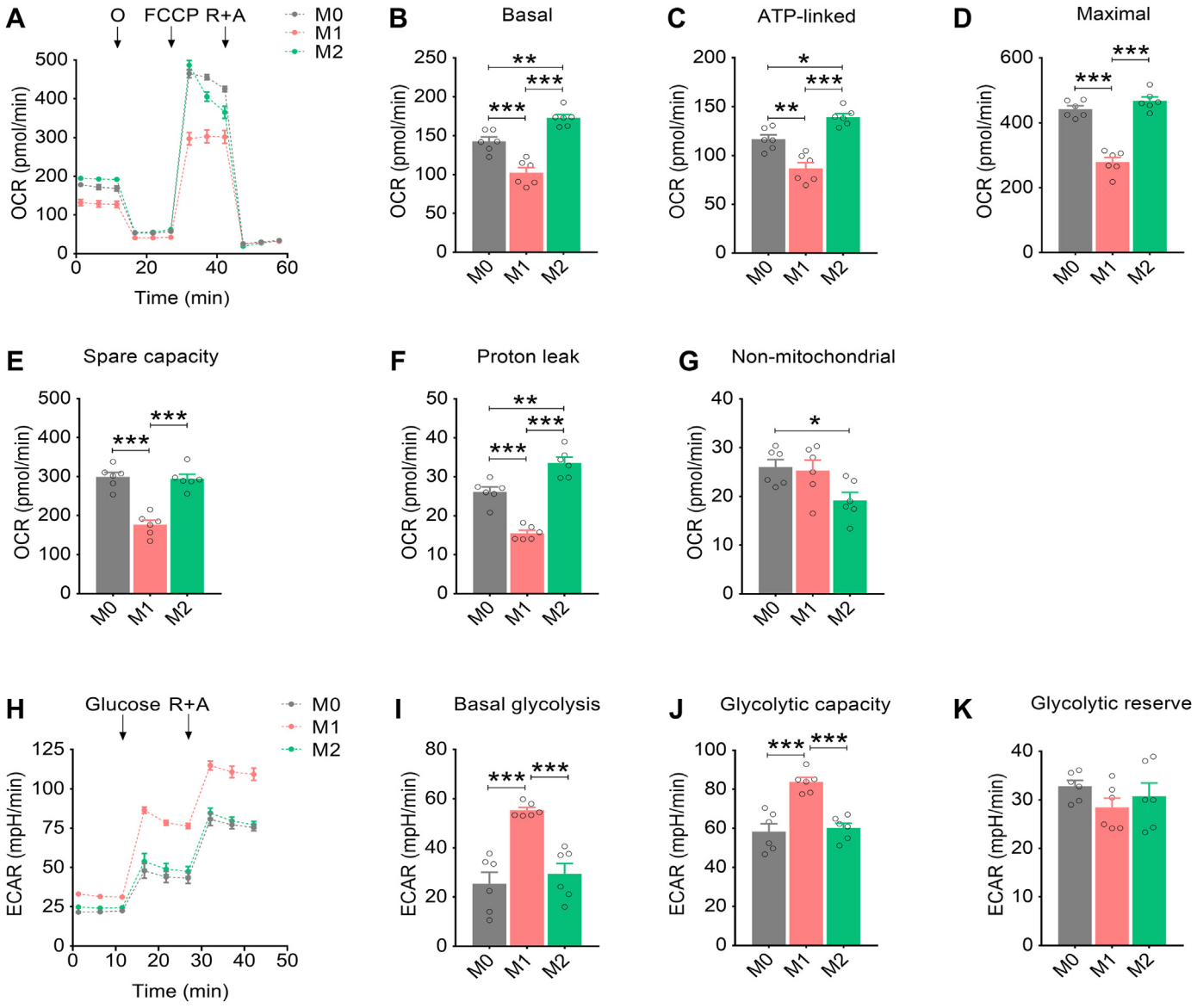


**Fig. 2. Macrophage metabolic profile depends on the inflammatory stimulus.** Average curves of OCR **(A)** and OCR-associated with different mitochondrial states **(B–G)** in naïve (M0) and M1/M2 polarized macrophages. Oligomycin (O), FCCP and rotenone plus antimycin-A (R + A). Average curves of ECAR **(H)** and ECAR-associated with different glycolytic states **(I–K)**. Six independent cell batches analyzed in triplicates. Data are expressed as mean ± SE. Statistical analyses were performed using one-way ANOVA followed by a Bonferroni's post-test. *, **, *** with $p < 0.05$, 0.01 and 0.001, respectively.

Because oxidants were generated in the extra-mitochondrial compartment, we evaluated the gene expression of phagocytic NADPH oxidase 2 (NOX2) and its regulatory subunits p40phox, p47phox and p67phox. Indeed, M1 macrophages showed markedly enhanced expression of NOX2 and regulatory subunits (Fig. 3G and H). In addition, M1 macrophages exhibited upregulation of RAC1 and 2 genes encoding proteins recruited to form the NADPH oxidase complex in the plasma membrane (Fig. 3I). These results show oxidants produced and released by M1 macrophages derives mostly from NOX2 and SOD1 activity.

### 3.4. *Pro-inflammatory stimulus reduces ER-mitochondria interaction and upregulate genes involved in mitochondrial dynamics*

We evaluated ER-mitochondria interaction using IP3R1-VDAC1 contact sites as previously described [12]. To test the efficiency of this technique, macrophages were treated with small interfering RNA (siRNA) to reduce VDAC1 or ITPR1 gene expression. In fact, we observed 82% reduction in VDAC1 and 73% reduction in ITPR1 mRNA levels when compared to control cells (Figs. S2A and B). As a consequence, the knocked down macrophages showed a 33% decrease in IP3R1-VDAC1 interaction sites when compared to control cells (Figs. S2C and D).

Next, we evaluated IP3R1-VDAC1 interaction sites after M1 or M2 stimuli. M1 macrophages showed 35% less IP3R1-VDAC1 interaction sites than M0 and M2. IP3R1-VDAC1 contact sites were equivalent in M0 and M2 (Fig. 4A and B).

We also tested whether M1 or M2 stimuli would affect mitochondrial dynamics related gene expression. M1 macrophages showed marked enhanced gene expression (6–10-fold) of both mitochondrial fusion (MFN1, MFN2 and OPA1) and fission (DRP1 and FIS1) markers when compared to M0. M2 macrophages had no significant alterations in MFN1 and MFN2, but also showed

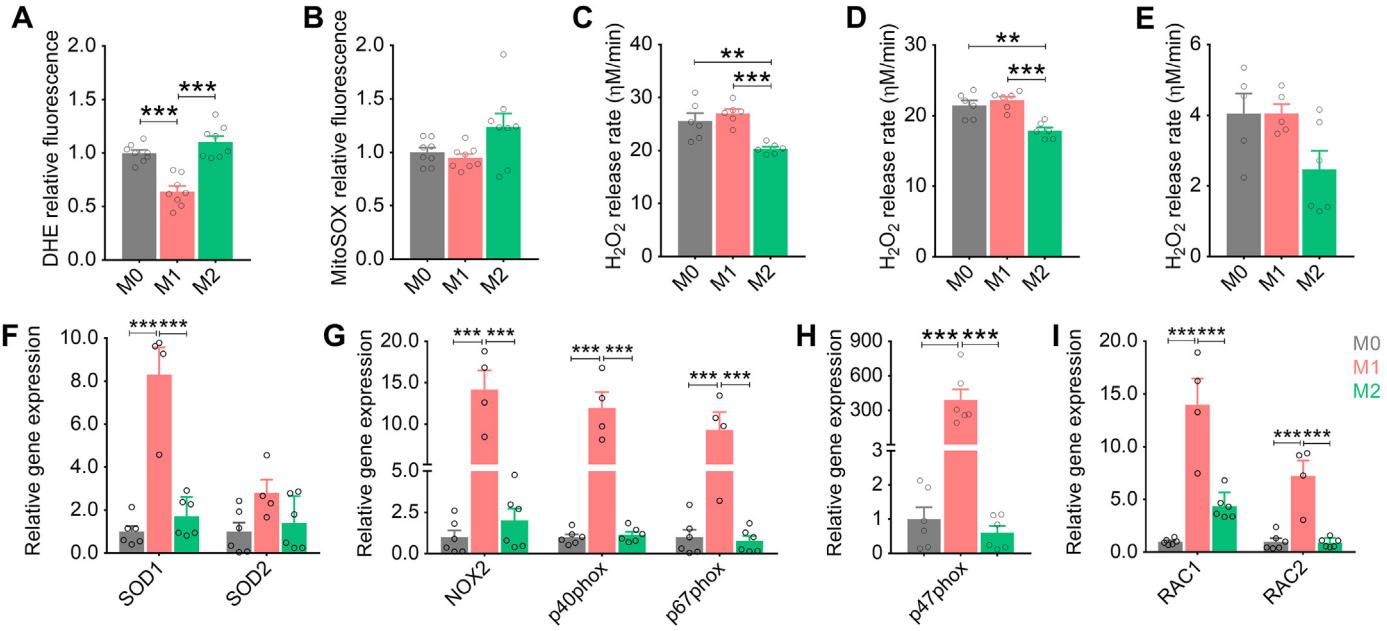


**Fig. 3. Inflammatory stimuli modulate oxidants production in macrophages.** Detection of superoxide anion production from whole-cell (DHE) **(A)** and mitochondria-derived (MitoSOX) **(B)**. Eight independent cell batches analyzed in triplicates. Quantitation of hydrogen peroxide ($H_2O_2$) release rate from whole-cell **(C)**, non-mitochondrial **(D)** and mitochondrial **(E)**. Six independent cell batches analyzed in triplicates. Expression of genes related to oxidant generators **(F–I)**. Four to six independent cell batches analyzed in duplicates. Data are expressed as mean ± SE. Statistical analyses were performed using one-way ANOVA followed by Bonferroni's post-test. **, *** with $p < 0.01$ and 0.001, respectively.

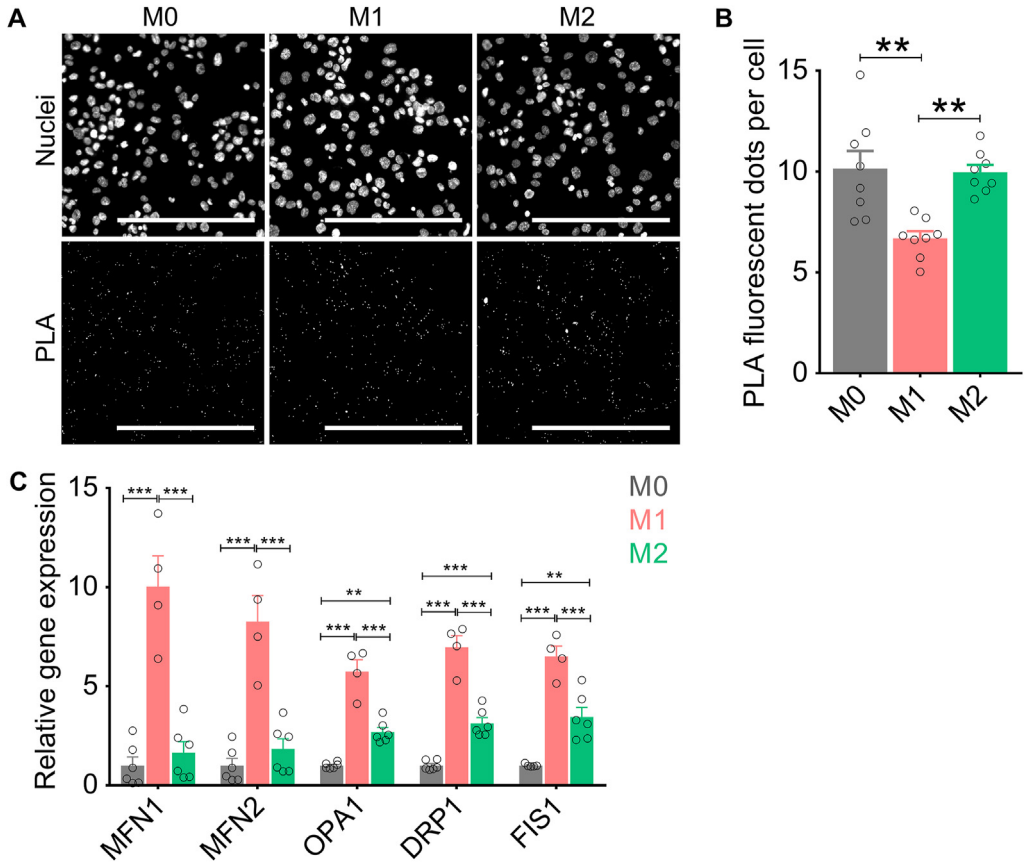


**Fig. 4. M1 macrophages show reduced ER-mitochondria interaction and upregulated mitochondrial fusion and fission markers. (A)** Representative images at 40x magnification and **(B)** quantitative analysis of IP3R1-VDAC1 interaction in naïve (M0) and M1/M2 polarized macrophages. IP3R1-VDAC1 interaction was detected using PLA and further labeled with Cyanine 5 (white dots). Nuclei were stained with DAPI (white spots). Scale bar = 100 μm. Eight independent cell batches analyzed in duplicates. (C) Relative expression of genes involved in mitochondrial fusion and fission. Four to six independent cell batches analyzed in duplicates. Data are expressed as mean ± SE. Statistical analyses were performed using one-way ANOVA followed by a Bonferroni's post-test. **, *** with $p < 0.01$ and 0.001, respectively.

increased fusion (OPA1) and fission (DRP1 and FIS1) mRNA levels, although in a much lower extend (about 3-fold) (Fig. 4C). These results show M1 macrophages present reduced ER-mitochondria interaction and increased mitochondria-mitochondria interactions due to increased expression of genes encoding mitochondrial fusion-fission regulatory proteins.

## 4. Discussion

Intracellular organelles interactions are hubs for overall cell signaling [13]. Here we hypothesized that metabolic and redox switches in polarized macrophages are associated with rearrangements in the ER-mitochondria interaction pattern. In fact, we showed LPS + IFNγ pro-inflammatory stimuli increased glycolytic metabolism, superoxide to hydrogen peroxide conversion and reduced the number of ER-mitochondria contact sites in M1 macrophages. While M1 macrophages present exacerbated glycolytic activity, M2 macrophages exhibited greater mitochondrial oxidative metabolism, reduced hydrogen peroxide release without significant effect on ER-mitochondria interaction. In addition, present findings suggest that the phenotype switch also interferes with the mitochondria-mitochondria interactions, once the mitochondrial fusion-fission related genes were markedly increased by pro-inflammatory stimuli.

M1 macrophages use glycolysis as the major source of ATP [14]. Macrophages activated via LPS/TLR pathway have enhanced glucose uptake, glycolysis and pentose phosphate pathways meanwhile oxidative phosphorylation and tricarboxylic acid cycle (TCA) are reduced [15,16]. On the other hand, the molecular mechanism underlying macrophage activation by cytokines IL4 and IL13 is not so clear, but oxidative phosphorylation overcomes glycolysis [17]. In fact, LPS + IFNγ pro-inflammatory treatment decreased mitochondrial respiration rates in macrophages when compared to naïve M0 or M2 macrophages. The OCR was reduced in all conditions: basal, phosphorylating and maximal stimulated (FCCP) respiration. Conversely, IL4+IL13 stimuli (M2) increased OCR in baseline and phosphorylating conditions and reduced OCR from non-mitochondrial sources compared with naïve M0 macrophages. Glycolysis and glycolytic capacity were increased in M1 macrophages and not changed in M2 as compared with M0 macrophages.

Macrophage polarization affects redox homeostasis. LPS + IFNγ stimuli decreased superoxide anion production and increased hydrogen peroxide release in macrophages. We excluded mitochondria as a source of both oxidants and found NOX2 and SOD1 genes upregulated. This suggest NOX2 as the major source of superoxide anion and SOD1 as a pathway for hydrogen peroxide formation in M1 macrophages. Moreover, nitric oxide-derived species generated from inducible NO synthase (iNOS) activity in LPS + IFNγ stimulated macrophages may damage the mitochondrial electron transfer chain once they inactivate iron-sulfur-containing complexes I and II [18–20]. Excess of hydrogen peroxide may also lead to mitochondrial dysfunction in both in vivo and in vitro models [21–23]. Thus, excess of oxidants may be related with lower OCR observed in M1 macrophages.

ER-mitochondria proximity allows calcium flux towards mitochondria via the mitochondrial calcium uniporter [24]. Low calcium concentrations (~2 μM) inside the mitochondria are important for ATP synthase activity [25] and optimal functioning of TCA enzymes such as pyruvic dehydrogenase phosphatase, α-ketoglutarate and isocitrate NADH dehydrogenases [26–29]. Thus, in μM range, calcium speeds up mitochondrial aerobic metabolism. On the other hand, excessive calcium concentrations induce mitochondrial permeability transition, followed by cell death [23]. Recent work showed that blood monocyte ($CD14^+$)-derived macrophages from patients carrying rheumatoid arthritis or coronary artery disease present increased ER-mitochondria cooperation, mitochondrial calcium influx and mitochondrial OCR when compared to macrophages from control subjects [4]. Because we found reduced ER-mitochondria interaction and OCR in LPS + IFNγ stimulated macrophages, we suggest reduced mitochondrial calcium uptake may be present in M1 macrophages, contributing to reduce oxidative metabolism.

We also showed pro-inflammatory stimulation of macrophages induces a pronounced upregulation of both mitochondrial fusion (MFN1/2 and OPA1) and fission (DRP1 and FIS1) related genes while anti-inflammatory stimulation induced mild changes in OPA1, DRP1 and FIS1 expression. Mitochondrial fusion-fission dynamics may be reciprocally regulated by the cell redox state and metabolism [30]. Both reactive nitrogen (RNS) and oxygen (ROS) species are connected with alterations in mitochondrial morphology, albeit in a cell- and context-dependent manner [30]. Mild oxidative stress has been shown to promote disulfide-mediated dimerization of MFN molecules, thus driving organelle tethering and subsequently fusion [31], while excessive ROS signaling leads to mitochondrial fission [30]. In addition, reciprocal crosstalk between mitochondrial dynamics and metabolism has been demonstrated [32]. While an overall view links mitochondrial fusion and fission to catabolic and anabolic states, respectively, other opposing evidences have also been reported [32]. Here, we suggest that both redox and metabolic shifts upon inflammatory stimuli drive reshapes of mitochondrial network. Finally, since pro-inflammatory stimulation of macrophages decreases ER-mitochondrial interaction and, thus likely decreases calcium entry into the mitochondria, alterations in mitochondrial fusion-fission processes driven by calcium signaling [33] are anticipated.

In conclusion, this study reveals ER-mitochondria interaction as a novel feature of the macrophage immune, metabolic and redox profiles.

## Author contributions

LHPA and HCFO conceived and designed the study, interpreted data and wrote the manuscript. LHPA and GGD carried out experiments and analyzed data. HCFO supervised and coordinated the research. All authors contributed to the article and approved its final version.

## Funding

This work was supported by São Paulo Research Foundation, FAPESP (2017/17728-8 and 2013/50615-1); National Council for Scientific and Technological Development, CNPq (300937/2018-0); FAPESP post-doctoral fellowships 2017/03402-3 (LHPA) and 2017/02903-9 (GGD).

## Declaration of competing interest

The authors declare no conflicts of interest.

## Appendix A. Supplementary data

Supplementary data to this article can be found online at https://doi.org/10.1016/j.bbrc.2022.03.086.

## References

[1] P.J. Murray, Macrophage polarization, Annu. Rev. Physiol. 79 (2017) 541–566, https://doi.org/10.1146/annurev-physiol-022516-034339.
[2] G. Chinetti-Gbaguidi, S. Colin, B. Staels, Macrophage subsets in atherosclerosis,

Nat. Rev. Cardiol. 12 (2015), https://doi.org/10.1038/nrcardio.2014.173.
[3] S. Missiroli, S. Patergnani, N. Caroccia, G. Pedriali, M. Perrone, M. Previati, M.R. Wieckowski, C. Giorgi, Mitochondria-associated membranes (MAMs) and inflammation, Cell Death Dis. 9 (2018), https://doi.org/10.1038/s41419-017-0027-2.
[4] M. Zeisbrich, R.E. Yanes, H. Zhang, R. Watanabe, Y. Li, L. Brosig, J. Hong, B.B. Wallis, J.C. Giacomini, T.L. Assimes, J.J. Goronzy, C.M. Weyand, Hypermetabolic macrophages in rheumatoid arthritis and coronary artery disease due to glycogen synthase kinase 3b inactivation, Ann. Rheum. Dis. 77 (2018), https://doi.org/10.1136/annrheumdis-2017-212647.
[5] L.H.P. Assis, G.G. Dorighello, T. Rentz, J.C. Souza, A.E. Vercesi, H.C.F. Oliveira, In vivo pravastatin treatment reverses hypercholesterolemia induced mitochondria-associated membranes contact sites, foam cell formation, and phagocytosis in macrophages, Front. Mol.Biosci. (2022) 9, https://doi.org/10.3389/fmolb.2022.839428.
[6] M. Genin, F. Clement, A. Fattaccioli, M. Raes, C. Michiels, M1 and M2 macrophages derived from THP-1 cells differentially modulate the response of cancer cells to etoposide, BMC Cancer 15 (2015), https://doi.org/10.1186/s12885-015-1546-9.
[7] K.J. Livak, T.D. Schmittgen, Analysis of relative gene expression data using real-time quantitative PCR and the 2−ΔΔCT method, Methods 25 (2001), https://doi.org/10.1006/meth.2001.1262.
[8] L.J. Toime, M.D. Brand, Uncoupling protein-3 lowers reactive oxygen species production in isolated mitochondria, Free Radic. Biol. Med. 49 (2010) 606–611, https://doi.org/10.1016/j.freeradbiomed.2010.05.010.
[9] J. Schindelin, I. Arganda-Carreras, E. Frise, V. Kaynig, M. Longair, T. Pietzsch, S. Preibisch, C. Rueden, S. Saalfeld, B. Schmid, J.-Y. Tinevez, D.J. White, V. Hartenstein, K. Eliceiri, P. Tomancak, A. Cardona, Fiji: an open-source platform for biological-image analysis, Nat. Methods 9 (2012), https://doi.org/10.1038/nmeth.2019.
[10] A. Kadl, P.R. Sharma, W. Chen, R. Agrawal, A.K. Meher, S. Rudraiah, N. Grubbs, R. Sharma, N. Leitinger, Oxidized phospholipid-induced inflammation is mediated by Toll-like receptor 2, Free Radic. Biol. Med. 51 (2011) 1903–1909, https://doi.org/10.1016/j.freeradbiomed.2011.08.026.
[11] A. Kadl, A.K. Meher, P.R. Sharma, M.Y. Lee, A.C. Doran, S.R. Johnstone, M.R. Elliott, F. Gruber, J. Han, W. Chen, T. Kensler, K.S. Ravichandran, B.E. Isakson, B.R. Wamhoff, N. Leitinger, Identification of a novel macrophage phenotype that develops in response to atherogenic phospholipids via Nrf2, Circ. Res. 107 (2010) 737–746, https://doi.org/10.1161/CIRCRESAHA.109.215715.
[12] E. Tubbs, P. Theurey, G. Vial, N. Bendridi, A. Bravard, M.A. Chauvin, J. Ji-Cao, F. Zoulim, B. Bartosch, M. Ovize, H. Vidal, J. Rieusset, Mitochondria-associated endoplasmic reticulum membrane (MAM) integrity is required for insulin signaling and is implicated in hepatic insulin resistance, Diabetes 63 (2014) 3279–3294, https://doi.org/10.2337/db13-1751.
[13] A.J. Mouton, X. Li, M.E. Hall, J.E. Hall, Obesity, hypertension, and cardiac dysfunction novel roles of immunometabolism in macrophage activation and inflammation, Circ. Res. (2020) 789–806, https://doi.org/10.1161/CIRCRESAHA.119.312321.
[14] L.A.J. O'Neill, E.J. Pearce, Immunometabolism governs dendritic cell and macrophage function, J. Exp. Med. 213 (2016) 15–23, https://doi.org/10.1084/jem.20151570.
[15] E.M. Palsson-McDermott, A.M. Curtis, G. Goel, M.A.R. Lauterbach, F.J. Sheedy, L.E. Gleeson, M.W.M. van den Bosch, S.R. Quinn, R. Domingo-Fernandez, D.G.W. Johnston, J. Jiang, W.J. Israelsen, J. Keane, C. Thomas, C. Clish, M. Vander Heiden, R.J. Xavier, L.A.J. O'Neill, Pyruvate kinase M2 regulates Hif-1α activity and IL-1β induction and is a critical determinant of the warburg effect in LPS-activated macrophages, Cell Metabol. 21 (2015) 65–80, https://doi.org/10.1016/j.cmet.2014.12.005.
[16] G.M. Tannahill, A.M. Curtis, J. Adamik, E.M. Palsson-McDermott, A.F. McGettrick, G. Goel, C. Frezza, N.J. Bernard, B. Kelly, N.H. Foley, L. Zheng, A. Gardet, Z. Tong, S.S. Jany, S.C. Corr, M. Haneklaus, B.E. Caffrey, K. Pierce, S. Walmsley, F.C. Beasley, E. Cummins, V. Nizet, M. Whyte, C.T. Taylor, H. Lin, S.L. Masters, E. Gottlieb, V.P. Kelly, C. Clish, P.E. Auron, R.J. Xavier, L.A.J. O'Neill, Succinate is an inflammatory signal that induces IL-1β through HIF-1α, Nature 496 (2013) 238–242, https://doi.org/10.1038/nature11986.
[17] J. van den Bossche, L.A. O'Neill, D. Menon, Macrophage immunometabolism: where are we (going)? Trends Immunol. 38 (2017) 395–406, https://doi.org/10.1016/j.it.2017.03.001.
[18] J. van den Bossche, J. Baardman, N.A. Otto, S. van der Velden, A.E. Neele, S.M. van den Berg, R. Luque-Martin, H.J. Chen, M.C.S. Boshuizen, M. Ahmed, M.A. Hoeksema, A.F. de Vos, M.P.J. de Winther, Mitochondrial dysfunction prevents repolarization of inflammatory macrophages, Cell Rep. 17 (2016) 684–696, https://doi.org/10.1016/j.celrep.2016.09.008.
[19] G. Brown, V. Borutaite, Nitric oxide and mitochondrial respiration in the heart, Cardiovasc. Res. 75 (2007) 283–290, https://doi.org/10.1016/j.cardiores.2007.03.022.
[20] B. Chénais, H. Morjani, J.-C. Drapier, Impact of endogenous nitric oxide on microglial cell energy metabolism and labile iron pool, J. Neurochem. 81 (2002) 615–623, https://doi.org/10.1046/j.1471-4159.2002.00864.x.
[21] S.W. Ballinger, C. Patterson, C.-N. Yan, R. Doan, D.L. Burow, C.G. Young, F.M. Yakes, B. van Houten, C.A. Ballinger, B.A. Freeman, M.S. Runge, Hydrogen peroxide− and peroxynitrite-induced mitochondrial DNA damage and dysfunction in vascular endothelial and smooth muscle cells, Circ. Res. 86 (2000) 960–966, https://doi.org/10.1161/01.RES.86.9.960.
[22] J.A. Ronchi, T.R. Figueira, F.G. Ravagnani, H.C.F. Oliveira, A.E. Vercesi, R.F. Castilho, A spontaneous mutation in the nicotinamide nucleotide transhydrogenase gene of C57BL/6J mice results in mitochondrial redox abnormalities, Free Radic. Biol. Med. 63 (2013) 446–456, https://doi.org/10.1016/j.freeradbiomed.2013.05.049.
[23] A.E. Vercesi, R.F. Castilho, A.J. Kowaltowski, H.C.F. de Oliveira, N.C. de Souza-Pinto, T.R. Figueira, E.N.B. Busanello, Mitochondrial calcium transport and the redox nature of the calcium-induced membrane permeability transition, Free Radic. Biol. Med. 129 (2018), https://doi.org/10.1016/j.freeradbiomed.2018.08.034.
[24] K.J. Kamer, V.K. Mootha, The molecular era of the mitochondrial calcium uniporter, Nat. Rev. Mol. Cell Biol. 16 (2015) 545–553, https://doi.org/10.1038/nrm4039.
[25] P.R. Territo, V.K. Mootha, S.A. French, R.S. Balaban, Ca $^{2+}$ activation of heart mitochondrial oxidative phosphorylation: role of the $F_0/F_1$ -ATPase, Am. J. Physiol. Cell Physiol. 278 (2000) C423–C435, https://doi.org/10.1152/ajpcell.2000.278.2.C423.
[26] R.M. Denton, Regulation of mitochondrial dehydrogenases by calcium ions, Biochim. Biophys. Acta Bioenerg. 1787 (2009), https://doi.org/10.1016/j.bbabio.2009.01.005.
[27] J.G. McCormack, R.M. Denton, Role of calcium ions in the regulation of intramitochondrial metabolism. Properties of the Ca2+-sensitive dehydrogenases within intact uncoupled mitochondria from the white and brown adipose tissue of the rat, Biochem. J. 190 (1980) 95–105, https://doi.org/10.1042/bj1900095.
[28] R.G. Hansford, Relation between cytosolic free Ca2+ concentration and the control of pyruvate dehydrogenase in isolated cardiac myocytes, Biochem. J. 241 (1987) 145–151, https://doi.org/10.1042/bj2410145.
[29] R.G. Hansford, F. Castro, Role of Ca2+ in pyruvate dehydrogenase interconversion in brain mitochondria and synaptosomes, Biochem. J. 227 (1985) 129–136, https://doi.org/10.1042/bj2270129.
[30] P.H.G.M. Willems, R. Rossignol, C.E.J. Dieteren, M.P. Murphy, W.J.H. Koopman, Redox homeostasis and mitochondrial dynamics, Cell Metabol. 22 (2015) 207–218, https://doi.org/10.1016/j.cmet.2015.06.006.
[31] T. Shutt, M. Geoffrion, R. Milne, H.M. McBride, The intracellular redox state is a core determinant of mitochondrial fusion, EMBO Rep. 13 (2012) 909–915, https://doi.org/10.1038/embor.2012.128.
[32] A.S. Rambold, E.L. Pearce, Mitochondrial dynamics at the interface of immune cell metabolism and function, Trends Immunol. 39 (2018) 6–18, https://doi.org/10.1016/j.it.2017.08.006.
[33] G. Szabadkai, A.M. Simoni, K. Bianchi, D. de Stefani, S. Leo, M.R. Wieckowski, R. Rizzuto, Mitochondrial dynamics and Ca2+ signaling, Biochim. Biophys. Acta Mol. Cell Res. 1763 (2006) 442–449, https://doi.org/10.1016/j.bbamcr.2006.04.002.